Histone H3 lysine 36 methyltransferase Hypb/Setd2 is required for embryonic vascular remodeling

Ming Hu[a,1], Xiao-Jian Sun[a,b,1], Yuan-Liang Zhang[a,1], Ying Kuang[c,1], Chao-Quan Hu[d], Wei-Li Wu[a], Shu-Hong Shen[a], Ting-Ting Du[a], Hong Li[e], Fei He[f], Hua-Sheng Xiao[f], Zhu-Gang Wang[c], Ting-Xi Liu[a,g], He Lu[d], Qiu-Hua Huang[a,2], Sai-Juan Chen[a,b,2], and Zhu Chen[a,b,2]

[a]State Key Laboratory of Medical Genomics, Shanghai Institute of Hematology, Rui Jin Hospital, Shanghai Jiao Tong University School of Medicine, Shanghai 200025, China; [b]Shanghai Center for Systems Biomedicine, Shanghai Jiao Tong University, Shanghai 200240, China; [c]Shanghai Research Center for Model Organisms, Shanghai 201203, China; [d]Institut National de la Santé et de la Recherche Médicale U728, Pôle Franco-chinois en Génomique et Sciences du Vivant, Institut Universitaire d'Hématologie, Université de Diderot, Hôpital Saint Louis, 75010, Paris, France; [e]Laboratoire de Recherche MERCI (Micro-Environnement et Régulation Cellulaire Intégrée), EA 3829, Faculté de Médecine et de Pharmacie, Université de Rouen, 76183 Rouen, France; [f]National Engineering Center for Biochip at Shanghai, Shanghai 201203, China; and [g]Institute of Health Sciences, Shanghai Institutes for Biological Sciences, Chinese Academy of Sciences and Shanghai Jiao Tong University School of Medicine, Shanghai 200025, China

Contributed by Zhu Chen, December 28, 2009 (sent for review December 9, 2009)

HYPB is a human histone H3 lysine 36 (H3K36)–specific methyltransferase and acts as the ortholog of yeast Set2. This study explored the physiological function of mammalian HYPB using knockout mice. Homozygous disruption of *Hypb* impaired H3K36 trimethylation but not mono- or dimethylation, and resulted in embryonic lethality at E10.5-E11.5. Severe vascular defects were observed in the $Hypb^{-/-}$ embryo, yolk sac, and placenta. The abnormally dilated capillaries in mutant embryos and yolk sacs could not be remodeled into large blood vessels or intricate networks, and the aberrantly rounded mesodermal cells exhibited weakened interaction with endothelial cells. The embryonic vessels failed to invade the labyrinthine layer of placenta, which impaired the embryonic–maternal vascular connection. These defects could not be rescued by wild-type tetraploid blastocysts, excluding the possibility that they were caused by the extraembryonic tissues. Consistent with these phenotypes, gene expression profiling in wild-type and $Hypb^{-/-}$ yolk sacs revealed that the *Hypb* disruption altered the expression of some genes involved in vascular remodeling. At the cellular level, $Hypb^{-/-}$ embryonic stem cell–derived embryonic bodies, as well as in vitro–cultured human endothelial cells with siRNA-mediated suppression of *HYPB*, showed obvious defects in cell migration and invasion during vessel formation, suggesting an intrinsic role of *Hypb* in vascular development. Taken together, these results indicate that Hypb is required for embryonic vascular remodeling and provide a tool to study the function of H3K36 methylation in vasculogenesis/angiogenesis.

knockout mice | embryonic lethality | vasculogenesis | angiogenesis | capillary tubule formation

Development of multicellular organisms is an integral of successive processes, in which a single cell gives rise to numerous cell types that exert various functions and organize their relationships to form the adult body plan. To control the development, one of the most fundamental tasks of an organism is the spatial and temporal regulation of expression of thousands of genes (1). In addition to the mechanisms that transcription factors control gene expression through recognizing DNA elements and recruiting general transcription machinery, covalent modifications of histones mediated by families of enzymatic cofactors have emerged as key regulatory mechanisms of gene expression (2–4). These histone modifications regulate gene expression through recruiting/dispelling some protein complexes and through altering the accessibility of chromatin for transcription machineries (5). Moreover, they may serve as an epigenetic marking system that is responsible for establishing and maintaining the heritable programs of gene expression during cellular differentiation and organism development (6, 7).

HYPB (also known as HSPC069, SETD2, hSET2 and KMT3A) is a recently defined histone methyltransferase (HMT). The human *HSPC069* gene was originally isolated from hematopoietic stem/progenitor cells (8), and the encoded protein was also identified as a factor that interacts with the Huntington disease protein huntingtin (9). Our previous studies identified HYPB as a histone H3 lysine 36 (H3K36)–specific HMT that interacts with hyperphosphorylated RNA polymerase II (pol II) (10). HYPB acts as the human ortholog of the yeast Set2, and this orthologous group is also conserved in other eukaryotes (11). Members of this orthologous group contain a triplicate AWS-SET-PostSET domain that mediates the H3K36 HMT activity (10, 12), a C-terminal Set2 Rbp1–interacting (SRI) domain that mediates the interaction with pol II (10, 13), and a WW domain that likely mediates protein–protein interaction (14). In addition, within the human HYPB, we identified a novel transcriptional activation domain that is conserved in vertebrates (10), suggesting diverse functions of HYPB through evolution. Although Set2 is the sole H3K36 HMT in yeast, multiple mammalian H3K36 HMTs have been defined (5). Interestingly, siRNA knockdown of *Hypb* in murine fibroblasts led to a specific loss of H3K36 trimethylation (H3K36me3), suggesting that murine Hypb is a nonredundant, specific enzyme for H3K36me3, at least in this type of cell (15). However, it remained unclear whether the mammalian HYPB (and the H3K36 methylation) is required for any developmental processes.

In this study, we created knockout mice to explore the function of mammalian HYPB in the context of development. Homozygous disruption of *Hypb* resulted in embryonic lethality with severe defects in blood vessel development. Generally, formation of embryonic blood vessels is one of the most essential processes for mammalian embryogenesis (16). Failures of this process would lead to growth retardation, swelling of the pericardium, and finally death in utero during early organogenesis (17). We made an effort to detail the vascular defects in $Hypb^{-/-}$ embryos, yolk sacs, and placentas by means of extensive histological analyses and gene expression profiling. We also used the tetraploid complementation assay to examine the possibility that the phenotypes could be caused by extraembryonic tissues. Furthermore, in vitro cultured embryonic stem (ES) cell–derived embryonic bodies (EBs) and endothelial cells

Author contributions: M.H., X.-J.S., H.L., Q.-H.H., S.-J.C., and Z.C. designed research; M.H., Y.-L.Z., Y.K., C.-Q.H., W.-L.W., S.-H.S., T.-T.D., H.L., and F.H. performed research; X.-J.S., H.-S.X., Z.-G.W., and T.-X.L. analyzed data; and H.M., X.-J.S., Q.-H.H., S.-J.C. and Z.C. wrote the paper.

The authors declare no conflict of interest.

Data deposition: The microarray data have been deposited in the Gene Expression Omnibus (GEO) database, www.ncbi.nlm.nih.gov/geo (accession no. GSE10113).

[1]M.H., X.-J.S., Y.-L.Z., and Y.K. contributed equally to this work.

[2]To whom correspondence may be addressed. E-mail: zchen@stn.sh.cn, sjchen@stn.sh.cn, or HQH10632@rjh.com.cn.

This article contains supporting information online at www.pnas.org/cgi/content/full/0915033107/DCSupplemental.

were used to investigate the role of Hypb in vascular development at the cellular level.

Results

Disruption of *Hypb* Impairs H3K36me3 and Results in Embryonic Lethality. The mouse *Hypb* locus was disrupted by homologous recombination, and the targeting region was located in exons 4 and 5 that cover the SET domain (Fig. 1*A*). Resistant ES cells were screened by genomic PCR (Fig. S1*A*) and verified by Southern blot (Fig. 1*B*). RT-PCR was performed to determine the expression of the mutant *Hypb* gene (Fig. S1*B*) and the products were sequenced. The results indicate that the inserted TK-neo cassette disrupted the ORF of the *Hypb* gene, thus abolishing the SET domain and the downstream domains. Embryos from heterozygous crosses were collected and their genotypes were monitored with genomic PCR (Fig. 1*C*). Histone methylation states of the embryos were determined by Western blot; the results showed that H3K36me3, but not H3K36me1/2, was impaired by the *Hypb* disruption (Fig. 1*D*).

Although heterozygous mice were viable, no homozygous knockout pups were obtained from more than 30 littermates of heterozygous intercrosses (Table S1), indicating that the *Hypb* disruption causes embryonic lethality. To determine the developmental stages when the lethality occurred, embryos were collected and analyzed at different stages. As a result, $Hypb^{-/-}$ embryos up to E10.5 were observed with expected Mendelian frequency, whereas no viable $Hypb^{-/-}$ embryos beyond E10.5 (Table S1). The $Hypb^{-/-}$ embryos began to show growth retardation from E8.5 (Fig. 2*A*). The E10.5 $Hypb^{-/-}$ embryos displayed growth defects with underdeveloped head and branchial arches, as well as neural development defects including forebrain hypoplasia and unclosed neural tubes (Fig. 2*A c* and *d*). Other phenotypes of the $Hypb^{-/-}$ embryos include incomplete embryonic turning and failure of allantois to fuse with the chorion (Fig. 2*A d*).

Vascular Defects in *Hypb*$^{-/-}$ Embryos. A number of $Hypb^{-/-}$ embryos exhibited a congestive appearance in the head with disorganized and dilated veins and capillaries (Fig. 2*B a* and *b*). Some $Hypb^{-/-}$ embryos exhibited head edema in the unilateral or bilateral headfolds (Fig. 2*B c*). Meanwhile, pericardial effusion was also frequently observed in $Hypb^{-/-}$ embryos (Fig. 2*B d*). These phenotypes have been considered as a common manifestation of disrupted blood flow and osmotic imbalance (17). To examine the structure of vasculatures, we performed whole-mount immunohistochemistry (IHC) with an endothelial marker PECAM-1. In the PECAM-1–stained wild-type (WT) embryos, well-structured hierarchic organization of artery, vein, and capillary can be seen (Fig. 2*C a* and *c*). In contrast, the $Hypb^{-/-}$ embryos showed little evidence of intricate network of vessels; instead, abnormally dilated and irregularly shaped blood vessels were observed, especially in the head region (Fig. 2*C b* and *d*).

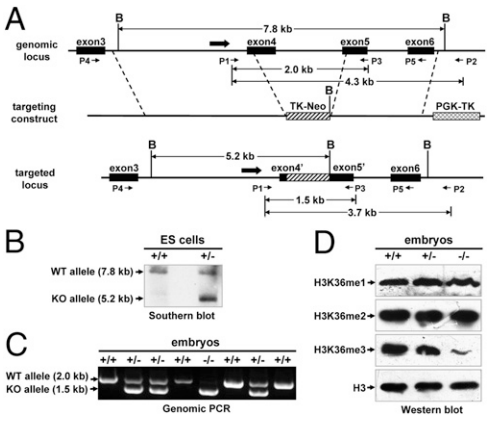

Fig. 1. Generation of *Hypb* knockout mice. (*A*) Schematic representation of the targeting strategy. The targeting region located in exons 4 and 5 is replaced with a TK-neo cassette. The remaining parts of exons 4 and 5 are denoted as exons 4′ and 5′. A reversed TK-PGK cassette is used for negative selection. A probe for Southern blot (boldface arrow) and five primers for PCR (thin arrows) are shown. B, restriction enzyme BamHI. (*B*) Southern blot analysis of targeted ES cells. (*C*) Genomic PCR analysis of embryos from heterozygous crosses with primers P1 and P3. (*D*) H3K36 methylation states of the embryos determined by Western blot with specific antibodies.

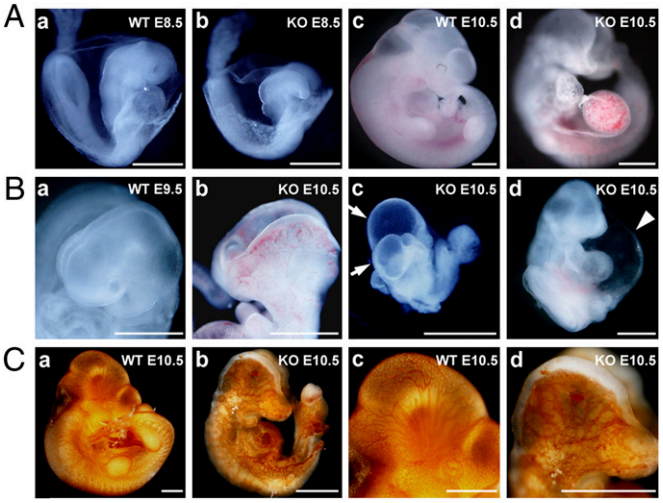

Fig. 2. Vascular defects in $Hypb^{-/-}$ embryos. (*A*) Morphology of wild-type (WT) and knockout (KO) embryos at E8.5 (*a* and *b*) and E10.5 (*c* and *d*). (*B*) Disorganized head veins and capillaries of E10.5 KO embryos (*b*) compared with E9.5 WT that is in similar developmental phase (*a*). E10.5 KO embryos exhibit head edemas (*c*, arrows) and pericardial edema and effusion (*d*, arrowhead). (*C*) Whole-mount IHC analysis of vasculatures with a PECAM-1 antibody. Magnifications in head regions of *a* and *b* are shown in *c* and *d*. (Scale bars, 600 μm.)

Vascular Defects in *Hypb*$^{-/-}$ Yolk Sacs. A striking phenotype observed in the extraembryonic tissues of $Hypb^{-/-}$ embryos was their pale and fragile yolk sacs. At E10.5, the WT yolk sacs exhibited a well-organized vascular network consisting of both capillaries and large vitelline vessels (Fig. 3*A a*), whereas in mutant littermates, the yolk sacs maintained poorly organized, dilated primitive capillaries but not large vitelline vessels (Fig. 3*A b*). Furthermore, the endodermal surfaces of the mutant yolk sacs were often ruffled, likely because of failure of the vasculatures to expand throughout the yolk sacs (Fig. 3*A b*). The structure of yolk sac vasculatures was examined by IHC with endothelial markers PECAM-1 and FLK-1. The WT yolk sacs showed well-structured hierarchical organization of large and small vessels (Fig. 3*B a* and *c*). In the $Hypb^{-/-}$ yolk sac, only a few dilated primitive capillaries were observed, whereas the large areas of continuous stainings suggested the inability of endothelial cells to form large vessels (Fig. 3*B b* and *d*). This phenotype was further analyzed by staining the erythrocytes with *o*-dianisidine, and the results showed abnormal aggregations of blood cells in the mutant yolk sacs (Fig. 3*B e* and *f*), also reflecting the disorganized vasculatures.

Section analyses provided more detailed evidences for the vascular defects. Well-circumscribed small vessels with tight endothelial cell linings were clearly observed in the WT yolk sacs (Fig. 3*C a*), whereas the vessels of $Hypb^{-/-}$ yolk sacs were characterized by dramatically increased cavities; visceral endoderm and mesoderm were widely separated with fewer attachments (Fig. 3*C b*). Meanwhile, cellular morphological changes in the $Hypb^{-/-}$ yolk sacs were also observed. Although the normal

DEVELOPMENTAL BIOLOGY

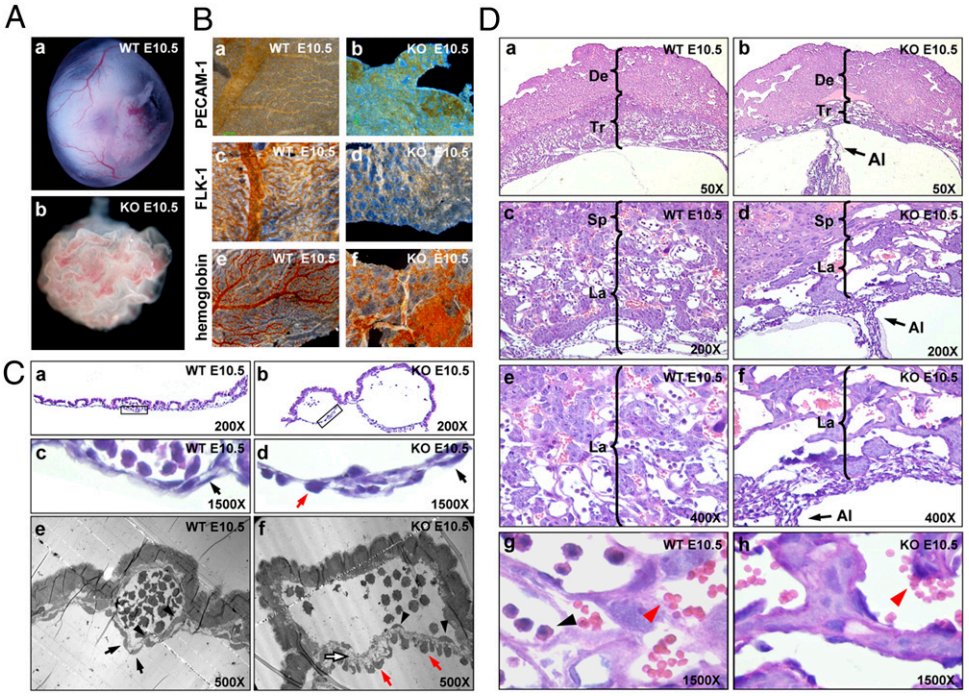

Fig. 3. Vascular defects in *Hypb*$^{-/-}$ yolk sacs and placentas. (*A*) Morphology of E10.5 WT (*a*) and KO (*b*) yolk sacs. (*B*) IHC and hemoglobin staining. (*a–d*) immunostaining with endothelial specific markers PECAM-1 and FLK-1. (*e* and *f*) O-dianisidine staining of hemoglobin in erythrocytes. (*C*) Histological and ultrastructural section analyses. (*a–d*) Histological analysis of the yolk sac sections. Areas indicated by c and d present magnifications of the marked areas in *a* and *b*. Black arrows denote normal, flattened appearance mesoderm cells, and the red arrows denote abnormally rounded mesoderm cells. (*e* and *f*) Ultrastructural analysis of the yolk sac sections using transmission electron microscope. Black arrowheads denote endothelial cells. White arrow denotes increased space between the endoderm and mesoderm cells in KO yolk sacs. (*D*) Defective labyrinthine layer architecture of KO placenta. H&E-stained sections of E10.5 WT and KO placentas are presented at various magnifications. Red and black arrowheads denote maternal mature erythrocytes and embryonic nucleated erythrocytes, respectively. Al, allantois; De, maternal decidua; La, labyrinthine layer; Sp, spongiotrophoblast layer; Tr, trophoblast layer.

visceral mesoderm cells display a stretched and flattened appearance (Fig. 3*C c,* black arrow), some mesoderm cells in the *Hypb*$^{-/-}$ yolk sacs are abnormally rounded (Fig. 3*C d,* red arrow). Ultrastructural analyses of the sections confirmed the morphological changes of the mesoderm cells (Fig. 3*C e* and *f,* black and red arrows). Furthermore, it is worthwhile to note that the spaces between the endothelial and mesoderm cells in the mutant yolk sac were significantly increased and were filled with dispersed collagen-like fibers (Fig. 3*C f,* white arrow).

Defective Labyrinthine Layer Architecture of *Hypb*$^{-/-}$ Placenta. Because vascularization is required for establishment of the transplacental exchange, vascular defects in the yolk sac should be associated with concomitant defects in the labyrinthine layer of placental vasculature (18). To address this issue, we examined the vasculatures in WT and *Hypb*$^{-/-}$ placentas. As seen in the WT placenta at E10.5, the labyrinthine layer developed well, and blood vessels containing nucleated erythrocytes invaded and interdigitated into the labyrinthine layer of the placenta (Fig. 3*D a, c, e,* and *g*). In contrast, a significant decrease in the thickness of the labyrinthine layer was observed in the E10.5 *Hypb*$^{-/-}$ placentas, although their spongiotrophoblast layers looked normal (Fig. 3*D b* and *d*). Meanwhile, the embryonic vessels remained at the periphery and did not invade into the labyrinthine layer (Fig. 3*D b* and *d*). Accordingly, although both maternal mature erythrocytes (red arrowhead) and embryonic nucleated erythrocytes (black arrowhead) were observed in WT placenta (Fig. 3*D g*), only maternal erythrocytes in *Hypb*$^{-/-}$ placenta (Fig. 3*D h*). Thus, the labyrinthine layer of *Hypb*$^{-/-}$ placentas consisted of trophoblast component alone but lacked the intricate network of branching embryonic vessels. These observations suggest that *Hypb* is important of vascular development in both extraembryonic components and embryo proper.

WT Tetraploid Extraembryonic Tissue Cannot Rescue *Hypb*$^{-/-}$ Phenotypes. To determine whether the *Hypb*$^{-/-}$ phenotypes could be caused by the defects of extraembryonic trophoblast tissue, we generated tetraploid chimeric mice by using WT tetraploid blastocysts to aggregate with the *Hypb*$^{-/-}$ diploid embryos. In this assay, we found that the *Hypb*$^{-/-}$ embryos with tetraploid extraembryonic tissues still died and exhibited similar defects in yolk sac and in intraembryonic vascularization (Table S2 and Fig. S2). These results suggested that the defects in placental vascularization are the allantoic mesoderm–derived vascular components rather than the extraembryonic trophoblasts.

***Hypb* Disruption Alters Expression of Genes Involved in Vascular Remodeling.** To verify the phenotypes and to understand the underlying mechanisms, we performed a gene expression profile of WT and *Hypb*$^{-/-}$ yolk sacs. We initially analyzed E10.5 yolk sacs. As a result, a total of 1,149 genes were identified as being significantly altered, with 633 being up-regulated and 516 being down-regulated. Among them, of note were 34 vasculogenic genes (Fig. 4*A*). To confirm these results and to quantify the gene expression changes, some genes were further analyzed with quantitative RT-PCR (RT-qPCR). The results were highly consistent with the microarray data (Fig. 4 *B* and *C*). Notably, some genes playing important roles in intercellular interaction and/or cell migration during vascular remodeling, including 10 secreted factor genes (*Ang*, *Angptl3, Angptl6*, *Ctgf, Cyr61, Igf1*, *Pdgfc*, *Plg*, *Serpinf1,* and *Vegfb*) and 8 membrane protein genes (*Cav1*, *Flt1*, *Gja4*, *Lama1*, *Lama4*, *Rhob*, *Sema3c,* and *Serpine1*), were significantly changed in *Hypb*$^{-/-}$ yolk

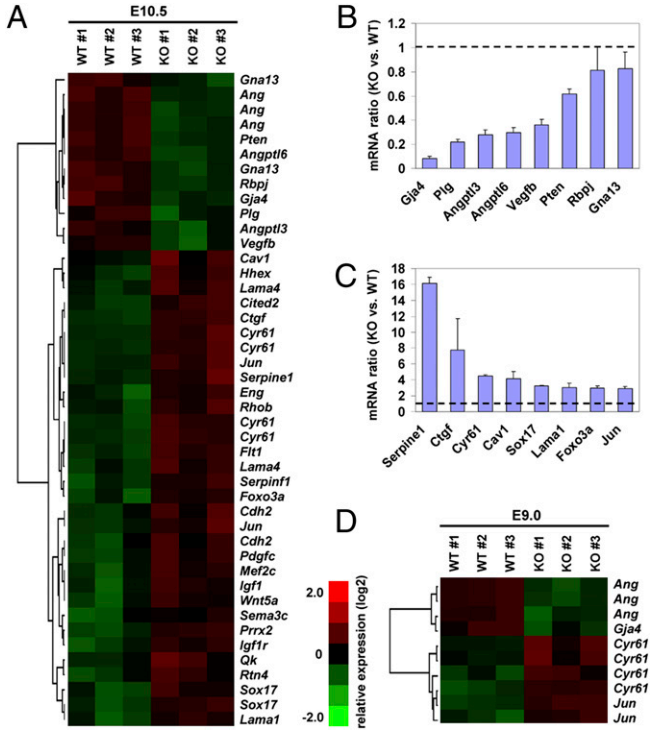

Fig. 4. Vasculogenic gene expression profile in WT and *Hypb*$^{-/-}$ yolk sacs. (*A*) Altered expression of vasculogenic genes in WT and KO E10.5 yolk sacs. Three independent experiments were noted as numbers 1, 2, and 3. The 34 genes were represented by 44 probe sets. Color bar indicates relative expression levels. (*B* and *C*) RT-qPCR analysis of representative vasculogenic genes that are down-regulated (*B*) or up-regulated (*C*) by *Hypb* disruption. Two independent experiments were performed; bar graphs represent average values. Dashed lines denote normalized expression levels of each gene in WT yolk sacs. (*D*) Altered expression of four vasculogenic genes (represented by 10 probe sets) in WT and KO E9.0 yolk sacs.

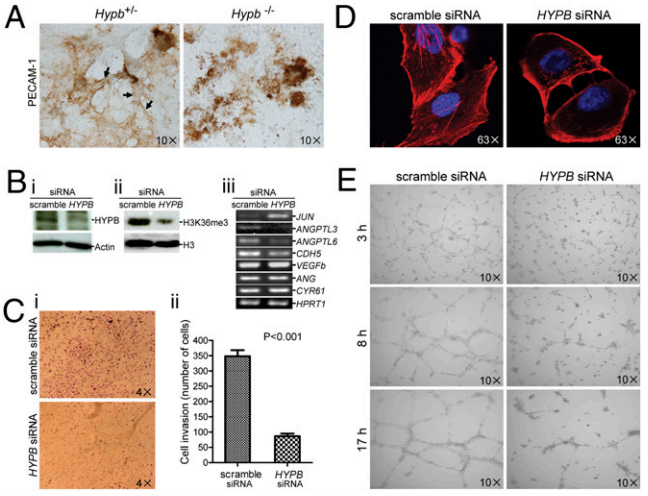

Fig. 5. Angiogenic defects in *Hypb*$^{-/-}$ EBs and *HYPB*-knockdown endothelial cells. (*A*) PECAM-1 staining of the endothelial cells in *Hypb*$^{+/-}$ and *Hypb*$^{-/-}$ EBs at day 23 postseeding on gelatin-coated cover glasses. Arrows denote well-formed vessels. (*B*) Decrease in HYPB protein (*i*) and H3K36me3 (*ii*) on the effect of *HYPB* siRNA. Western blots were performed 72 h after siRNA treatment. (*iii*) RT-PCR analyses of a few angiogenesis-related genes in *HYPB*-knockdown endothelial cells; *HPRT1* gene was used as control. (*C*) Cell invasion assays using transwell Boyden chambers (*i*) or Matrigel where invading cells were counted and quantified (*ii*). (*D*) Detection of F-ACTIN using rhodamine–phalloidin staining at 48 h after siRNA treatment. Representative confocal images were shown at 63/1.4× oil DIC objective. (*E*) Capillary tubule formation on Matrigel with full medium. Cells were photographed with 10× magnification at different time points.

sacs (Fig. 4*A*–*C*), which is largely consistent with the poor interaction of the endothelial cells with surrounding cells and matrix (Fig. 3*C*). We also checked some hematopoietic genes, especially the genes involved in erythropoiesis that are active in mouse yolk sacs (19). Although observing a slight down-regulation of the erythrocyte membrane protein band 4.2 gene *Epb4.2* in the *Hypb*$^{-/-}$ yolk sac, we did not find significant alteration of the important hematopoietic/erythropoietic genes (e.g., *Runx1*, *Scl/Tal1*, *Lmo2*, *Gata2*, *Pu.1/Sfpi1*, *Cebpα*, *Nfe2*, *Gata1*, *Fog/Zfpm1*, *Klf1*, and *Alas2*, and embryonic hemoglobin genes *Hbb-y*, *Hbb-bh1*, and *Hba-x*), suggesting that the hematopoiesis of the *Hypb*$^{-/-}$ yolk sac was not severely defective at this stage. Next, we analyzed the gene expression patterns of E9.0 yolk sacs. This analysis was expected to be potent for identification of some primary genes that contribute to the vascular defects, because the *Hypb*$^{-/-}$ yolk sacs at this stage had not shown apparent defects. Notably, four vasculogenic genes (*Ang*, *Gja4*, *Cyr61,* and *Jun*) were consistently regulated by the *Hypb* disruption at both E9.0 and E10.5 stages (Fig. 4*D*). Thus, we speculate that misregulations of these genes are among the earliest events leading to the severe vascular defects of the *Hypb*$^{-/-}$ mice.

***Hypb* Is Required for Vessel Formation in ES Cell–Derived EBs.** To prove the role of Hypb in vascular development, we differentiated *Hypb*$^{+/-}$ and *Hypb*$^{-/-}$ ES cells into EBs, which recapitulate some processes of early embryogenesis including the formation of vascular plexus, thus providing an ideal in vitro model system to study the mechanisms of vascular development (20). At day 23 of differentiation, the endothelial cells were revealed by PECAM-1 staining in both *Hypb*$^{+/-}$ and *Hypb*$^{-/-}$ EBs (Fig. 5*A*); however, the vessel formation in the *Hypb*$^{-/-}$ EBs was significantly impaired (Fig. 5*A*, *Right*) compared with the *Hypb*$^{+/-}$ EBs, which retained normal activity (Fig. 5*A*, *Left*).

Knockdown of *HYPB* in Human Endothelial Cells Impairs Migration and Tubule Formation Activities. To further elucidate the cellular mechanism by which *HYPB* contributes to vascular development, we sought to determine whether *HYPB* plays a role in the mobility and the angiogenic activity of endothelial cells. For this purpose, we transiently transfected human microvascular endothelial cells (HMEC-1) with *HYPB* siRNA, and a scramble siRNA was used as a control. Consistent with the knockout mouse data, knockdown of *HYPB* significantly reduced H3K36me3 in the HMEC-1 cells (Fig. 5*B*). Cell invasion assays indicated that *HYPB* siRNA–transfected cells showed an approximately fourfold decrease in the number of invasive cells, compared with the control cells (Fig. 5*C*). Given that endothelial cell migration requires actin reorganization, we analyzed the filamentous actin (F-ACTIN) in the HMEC-1 cells. The results indicated that *HYPB*-knockdown led to disorganized F-ACTIN stress fibers and defective formation of lamellipodia (Fig. 5*D*), which is consistent with the impaired mobility of these cells. Moreover, we used an in vitro tube formation assay to examine the capability of the cells to form capillary-like tubes on the Matrigel, regarded as representative morphogenesis of the later stage of angiogenesis (21). Consistent with the observations in embryos, whereas the control cells formed tubule networks with tightly junctions over a 17-h culture (Fig. 5*E*, *Left*), the *HYPB*-knockdown dramatically abrogated this activity (Fig. 5*E*, *Right*). Thus, these results suggest an autonomous effect of *HYPB* suppression in endothelial cell angiogenesis. We also checked, in the *HYPB*-knockdown endothelial cells, the mRNA levels of seven angiogenesis-related genes as compared with those in *Hypb*$^{-/-}$ yolk sac by using RT-PCR analyses. Notably, the expression of *c-JUN, ANGPTL3, and ANGPTL6* was

indeed altered in the same pattern as in *Hypb*$^{-/-}$ yolk sacs. Nevertheless, the other four genes displayed a distinct pattern, with no changes seen in *CYR61, ANG, and VEGFb* whereas they were either up-regulated (*Cyr61*) or down-regulated (*Ang and Vegfb*) in *Hypb*$^{-/-}$ yolk sacs; with regard to *CDH5*, a down-regulation was observed although its expression was not modulated in *Hypb*$^{-/-}$ yolk sacs (Fig. 5*B iii;* also Fig. 4 for comparison).

Discussion

In this study, our objective was to investigate the physiological function of Hypb in the context of development. We observed that the *Hypb*$^{-/-}$ mice did not exhibit any distinguishable defects in morphology and histology until E8.5, when they began to exhibit growth retardation. This observation suggests that the earlier developmental processes are not affected by the *Hypb* disruption and that *Hypb* may not be required for some basic cellular functions. Of note, our studies suggest that *Hypb* may play a relatively specific role in embryonic vascular development. During embryogenesis, the blood vessels arise from endothelial precursors, which share an origin with hematopoietic progenitors, therefore termed hemangioblasts (22, 23). Despite obvious defects of the vasculature and circulation in the *Hypb*$^{-/-}$ mice, the red blood cells were consistently observed in the mutant yolk sacs and embryos, and the *o*-dianisidine staining experiment revealed the existence of functional hemoglobin in the erythrocytes. Furthermore, gene expression profile indicates that many important hematopoietic genes are not affected by the *Hypb* disruption. These observations demonstrate normal differentiation and maturation of erythrocytes in the mutant mice and suggest that the disruption of *Hypb* may primarily disturb the development of blood vessels rather than the red blood cells per se at the embryonic stage.

In mammalian embryos, formation of the vascular system is implemented by two distinct processes, namely, vasculogenesis and angiogenesis (24). During vasculogenesis, the hemangioblasts differentiate into endothelial cells to form the primitive vascular plexus; during angiogenesis, the vascular plexus progressively expands and remodels into a highly organized mature vascular network. Whereas vasculogenesis occurs only in embryogenesis, angiogenesis contributes to the normal growth of both embryonic and postnatal tissues and in pathological situations such as wound healing and cancer (25). Our results provide evidences supporting that the endothelial cell differentiation and vasculogenesis occur in the *Hypb*$^{-/-}$ mice. The endothelial cells were consistently detected in *Hypb*$^{-/-}$ yolk sacs by IHC and section analysis, as well as in *Hypb*$^{-/-}$ ES cell–derived EBs. Furthermore, microarray and RT-PCR analyses revealed that the important regulators of vasculogenesis (e.g., *Scl/Tal1*, *Vezf1*, *Ets1*), as well as the markers for differentiated endothelial cells (e.g., *Pecam-1*, *Kdr/Flk-1*) presented in the mutant yolk sacs without obvious alteration. In contrast, vessel growth and maturation of *Hypb*$^{-/-}$ mice appears to be impaired at an early stage. The *Hypb*$^{-/-}$ embryos and yolk sacs were observed to possess primitive capillaries but not large vessels, suggesting that the *Hypb* disruption prevent tissue remodeling of the capillaries as well as further vessel development. Remarkably, both histological and ultrastructural analyses of the sections of the mutant yolk sacs revealed abnormally rounded mesodermal cells and increased space between mesodermal and endothelial cells, which likely weaken the interaction between these cells and prohibit appropriate stabilization of the vasculatures by recruitment of surrounding cells (26). The expanded sheets of endothelial cells observed in the *Hypb*$^{-/-}$ yolk sacs are likely due to the fusion of the unstable capillaries that hardly form connections (pillars) between two layers of the yolk sac. Consistent with these in vivo phenotypes, in vitro cultured endothelial cells with suppression of *HYPB* showed impaired migration and vessel formation activities, suggesting an endothelial cell–intrinsic function of *HYPB* and at least partially explaining the failure of vascular remodeling in *Hypb*$^{-/-}$ mice. Of note, the modulation of mRNA levels of *c-JUN, ANGPTL3,* and *ANGPTL6* genes in *HYPB* knock-down human endothelial cells was similar to that in *Hypb*$^{-/-}$ yolk sac in mice. The difference in the modulation pattern of some other genes might reflect cells/tissues at distinct developmental stages in two different species. It remains to be studied whether *Hypb* also affects other aspects involved in the angiogenesis process, such as the recruitment of pericytes and smooth muscle cells during angiogenesis.

Consistent with these vascular anomalies observed in vivo and in vitro, gene expression profile in yolk sacs revealed that the some particular genes involved in angiogenesis were deregulated by *Hypb* disruption. The yolk sac offers particular advantages for the expression analysis of vasculogenic/angiogenic and hematopoietic genes because (*i*) it represents a major organ of vasculature and blood development during early embryogenesis (19); (*ii*) its organization is relatively simpler than the embryo proper (19); and (*iii*) apart from the vascular defects, the size and appearance of the *Hypb*$^{-/-}$ yolk sacs were not significantly affected by the growth retardation of the embryos at the stages analyzed. Among the altered genes, notably, a potent inducer of angiogenesis namely angiogenin (Ang) was consistently down-regulated by the *Hypb* disruption even at early developmental stages when the phenotypes had not been visible, which would arrest the normal angiogenesis induced by other angiogenic proteins such as FGFs, epidermal growth factor (EGF), and VEGF (27). Another significantly down-regulated gene *Gja4* encodes the gap junction protein α4 (also known as Connexin37). Gja4/Connexin37 protein and its homolog Gja5/Connexin40 are functionally expressed in endothelial cells and contribute to the endothelial–endothelial and endothelial–smooth muscle gap junction channels; in addition, ablation of both Gja4 and Gja5 in mice results in severe vascular abnormalities (28). Furthermore, several other factors (e.g., Angptl3, Angptl6, and Cyr61) implicated in cellular adhesion/migration (29–31) were also found to be consistently regulated by the *Hypb* disruption. Although it still remains to be determined whether these genes are direct or indirect targets of Hypb, these data suggest that Hypb may differentially regulate multiple genes/pathways involved in angiogenesis, and are useful for fully understanding the mechanisms of Hypb-mediated epigenic regulation in angiogenesis.

Besides HYPB, there are some other mammalian H3K36 HMTs (5). How do they regulate the H3K36 methylation and the expression of target genes in development? Our results indicate that mouse Hypb is required for H3K36me3 during embryogenesis; thus, H3K36me1/2 may be catalyzed by other H3K36 HMTs. Among these HMTs, NSD1-knockout mice failed to complete gastrulation, likely because of cell apoptosis and mesodermal defects (32). In contrast, Hypb appears to exert a distinct, more specific function in embryonic development. Considering that these HMTs have different domain architectures and possibly different expression patterns, it is reasonable to postulate that the different H3K36 HMTs play distinct roles and cooperate to subtly regulate histone methylation and gene expression, thus controlling complicated developmental processes. Although H3K36 methylation has been implicated in multiple molecular functions including transcriptional elongation, suppression of cryptic transcription and mRNA export (33–36), it remains unclear whether H3K36 methylation contributes to any specific developmental processes. In this study, we identified the genes altered by the *Hypb* disruption, some of which might be directly or indirectly related to the loss of H3K36me3, thus allowing study of potential functions of Hypb and H3K36 methylation on different genes. Furthermore, our results clearly suggest that the processes of mammalian vascularization (vasculogenesis and angiogenesis), which have been actively studied in vivo and in vitro for both basic research and cancer therapeutics (25), can be considered as major aspects to further explore the physiological function of Hypb and H3K36 methylation and to gain insights into the underlying mechanisms.

Materials and Methods

Generation of *Hypb* Knockout Mice. The targeting vector (XpPNT) of *Hypb* locus was electroporated into CJ-7 ES cells. The heterozygous ES cells were microinjected into C57BL/6 blastocysts, followed by implantation into pseudopregnant B6CBF1 foster mothers. Male chimeras were mated with C57BL/6 females to generate F1 mice, which were further bred to generate F2 progeny. The F1 offspring were backcrossed to the C57BL/6 and 129/Sv strains for multiple generations to examine the persistence of the phenotypes.

Embryo Dissection, Histology, and Transmission Electron Microscope Analyses. Embryos, yolk sacs, and placentas were fixed overnight in 4% paraformaldehyde and then subjected to paraffin embedding. Serial sections (4 μm) were cut, deparaffinized, and stained with H&E. A part of yolk sac or embryo for each assay was used for the genotyping. Staining of the PECAM-1 and the FLK-1 were performed using monoclonal antibodies MEC13.3 and Avas12α1 and detected with a HRP Detection Kit (BD Bioscience). The hemoglobin was stained with *o*-dianisidine (Sigma-Aldrich). For transmission electron microscope analysis, yolk sacs were fixed overnight in 2% glutaraldehyde, postfixed in 1% OsO_4 for 2 h, dehydrated in a graded series of ethanol, transferred into propylene oxide, and embedded in epon. Ultrathin sections were cut and examined using a Philips CM 120 transmission electron microscope.

Tetraploid Complementation Assay. Tetraploid complementation assay was performed as in *SI Text.*

Microarray and RT-qPCR. Microarray was performed with the Affymetrix GeneChip Mouse Genome 430 2.0 Arrays. qPCR was performed with the Custom Plating TaqMan Array Plates and a 7300 Real-Time PCR system (Applied Biosystems; details in *SI Text*). The microarray data have been deposited in the Gene Expression Omnibus with accession number GSE10113.

ES Cell Culture and EB Differentiation. ES cell culture and EB differentiation are discussed in *SI Text.*

siRNA Transfection and F-ACTIN Staining. siRNA sequences are given in *SI Text* (36). A 10 nM quantity of chemically synthesized siRNA was transfected using INTERFERin Reagent (Polyplus Transfection). Rhodamine-phalloidin (Cytoskeleton) was used to label F-ACTIN at 48 h post siRNA treatment.

Cell Invasion Assay. Cells were treated with siRNA for 48 h. Cells (2.5×10^4) were seeded into the Biocoat Matrigel invasion chamber (BD Bioscience). A 0.5-mL quantity of serum-free culture medium was added to the upper chamber. The lower chamber contained 10% FCS. The cells were allowed to invade for 24 h. Cells penetrated through the Matrigel to the underside surfaces of the membranes were fixed and stained with 1% toluidine blue.

Tubule Formation Assay. Tubule formation assay was performed as described previously (37). Briefly, HMEC-1 cells were transfected with siRNA for 24 h, and 4×10^4 trypsin-dissociated cells were resuspended in 0.5 mL fresh full medium and seeded into Matrigel-coated 24-well plates. Capillary tubules were observed at different time points over the next 24 h.

ACKNOWLEDGMENTS. We thank Drs. Xue-Jun Zhang (Shanghai Institutes for Biological Sciences, Shanghai, China) and Xiao Yang (Institute of Biotechnology, Beijing, China) for constructive discussion, and Dr. Ying Jin (Shanghai Stem Cell Institute, Shanghai, China) for construction of ES cells for the EB differentiation assay. We thank our colleagues at the Shanghai Institute of Hematology for their support and discussion. This work was supported in part by the National Natural Science Foundation of China (30671170); the Chinese National Key Basic Research Project (973, 2009CB825604, 2010CB529200); the National High Tech Program for Biotechnology (863, 2006AA02A405); the Key Discipline program of Shanghai Municipal Education Commission (Y0201); the Grant for Innovation Group of the National Natural Science Foundation of China (30821063); the Shanghai Municipal Commission for Science and Technology (06DZ2202, 07DZ05908, 08DZ2200100); the Special Foundation for Doctor Discipline of Ministry of Education (200602480696); the Institut de Cancer, Cancéropôle Île-de-France of France (PL06_130); and the Shanghai Jiao Tong University–Genzyme Postdoctoral Fellowship Program. M.H. is supported by the Innovation Foundation for Doctoral Student of Shanghai Jiao Tong University (BXJ0609).

1. Levine M, Davidson EH (2005) Gene regulatory networks for development. *Proc Natl Acad Sci USA* 102:4936–4942.
2. Strahl BD, Allis CD (2000) The language of covalent histone modifications. *Nature* 403: 41–45.
3. Jenuwein T, Allis CD (2001) Translating the histone code. *Science* 293:1074–1080.
4. Shi Y, Whetstine JR (2007) Dynamic regulation of histone lysine methylation by demethylases. *Mol Cell* 25:1–14.
5. Kouzarides T (2007) Chromatin modifications and their function. *Cell* 128:693–705.
6. Ayyanathan K, et al. (2003) Regulated recruitment of HP1 to a euchromatic gene induces mitotically heritable, epigenetic gene silencing: A mammalian cell culture model of gene variegation. *Genes Dev* 17:1855–1869.
7. Hansen KH, et al. (2008) A model for transmission of the H3K27me3 epigenetic mark. *Nat Cell Biol* 10:1291–1300.
8. Zhang QH, et al. (2000) Cloning and functional analysis of cDNAs with open reading frames for 300 previously undefined genes expressed in CD34+ hematopoietic stem/progenitor cells. *Genome Res* 10:1546–1560.
9. Faber PW, et al. (1998) Huntingtin interacts with a family of WW domain proteins. *Hum Mol Genet* 7:1463–1474.
10. Sun XJ, et al. (2005) Identification and characterization of a novel human histone H3 lysine 36-specific methyltransferase. *J Biol Chem* 280:35261–35271.
11. Sun XJ, et al. (2008) Genome-wide survey and developmental expression mapping of zebrafish SET domain-containing genes. *PLoS One* 3:e1499.
12. Strahl BD, et al. (2002) Set2 is a nucleosomal histone H3-selective methyltransferase that mediates transcriptional repression. *Mol Cell Biol* 22:1298–1306.
13. Kizer KO, et al. (2005) A novel domain in Set2 mediates RNA polymerase II interaction and couples histone H3 K36 methylation with transcript elongation. *Mol Cell Biol* 25:3305–3316.
14. Hesselberth JR, et al. (2006) Comparative analysis of Saccharomyces cerevisiae WW domains and their interacting proteins. *Genome Biol* 7:R30.
15. Edmunds JW, Mahadevan LC, Clayton AL (2008) Dynamic histone H3 methylation during gene induction: HYPB/Setd2 mediates all H3K36 trimethylation. *EMBO J* 27: 406–420.
16. Risau W, Flamme I (1995) Vasculogenesis. *Annu Rev Cell Dev Biol* 11:73–91.
17. Copp AJ (1995) Death before birth: Clues from gene knockouts and mutations. *Trends Genet* 11:87–93.
18. Rossant J, Cross JC (2001) Placental development: Lessons from mouse mutants. *Nat Rev Genet* 2:538–548.
19. Baron MH (2003) Embryonic origins of mammalian hematopoiesis. *Exp Hematol* 31: 1160–1169.
20. Ng YS, Ramsauer M, Loureiro RM, D'Amore PA (2004) Identification of genes involved in VEGF-mediated vascular morphogenesis using embryonic stem cell-derived cystic embryoid bodies. *Lab Invest* 84:1209–1218.
21. Staton CA, Reed MW, Brown NJ (2009) A critical analysis of current in vitro and in vivo angiogenesis assays. *Int J Exp Pathol* 90:195–221.
22. Choi K, Kennedy M, Kazarov A, Papadimitriou JC, Keller G (1998) A common precursor for hematopoietic and endothelial cells. *Development* 125:725–732.
23. Nishikawa SI, Nishikawa S, Hirashima M, Matsuyoshi N, Kodama H (1998) Progressive lineage analysis by cell sorting and culture identifies FLK1+VE-cadherin+ cells at a diverging point of endothelial and hemopoietic lineages. *Development* 125: 1747–1757.
24. Risau W, et al. (1988) Vasculogenesis and angiogenesis in embryonic-stem-cell-derived embryoid bodies. *Development* 102:471–478.
25. Carmeliet P (2005) Angiogenesis in life, disease and medicine. *Nature* 438:932–936.
26. Suri C, et al. (1996) Requisite role of angiopoietin-1, a ligand for the TIE2 receptor, during embryonic angiogenesis. *Cell* 87:1171–1180.
27. Kishimoto K, Liu S, Tsuji T, Olson KA, Hu GF (2005) Endogenous angiogenin in endothelial cells is a general requirement for cell proliferation and angiogenesis. *Oncogene* 24:445–456.
28. Simon AM, McWhorter AR (2002) Vascular abnormalities in mice lacking the endothelial gap junction proteins connexin37 and connexin40. *Dev Biol* 251:206–220.
29. Camenisch G, et al. (2002) ANGPTL3 stimulates endothelial cell adhesion and migration via integrin alpha vbeta 3 and induces blood vessel formation in vivo. *J Biol Chem* 277:17281–17290.
30. Oike Y, et al. (2004) Angiopoietin-related growth factor (AGF) promotes angiogenesis. *Blood* 103:3760–3765.
31. Babic AM, Kireeva ML, Kolesnikova TV, Lau LF (1998) CYR61, a product of a growth factor-inducible immediate early gene, promotes angiogenesis and tumor growth. *Proc Natl Acad Sci USA* 95:6355–6360.
32. Rayasam GV, et al. (2003) NSD1 is essential for early post-implantation development and has a catalytically active SET domain. *EMBO J* 22:3153–3163.
33. Keogh MC, et al. (2005) Cotranscriptional set2 methylation of histone H3 lysine 36 recruits a repressive Rpd3 complex. *Cell* 123:593–605.
34. Carrozza MJ, et al. (2005) Histone H3 methylation by Set2 directs deacetylation of coding regions by Rpd3S to suppress spurious intragenic transcription. *Cell* 123:581–592.
35. Yoh SM, Lucas JS, Jones KA (2008) The Iws1:Spt6:CTD complex controls cotranscriptional mRNA biosynthesis and HYPB/Setd2-mediated histone H3K36 methylation. *Genes Dev* 22:3422–3434.
36. Xie P, et al. (2008) Histone methyltransferase protein SETD2 interacts with p53 and selectively regulates its downstream genes. *Cell Signal* 20:1671–1678.
37. Pillé JY, et al. (2005) Anti-RhoA and anti-RhoC siRNAs inhibit the proliferation and invasiveness of MDA-MB-231 breast cancer cells in vitro and in vivo. *Mol Ther* 11: 267–274.